Auricular surface morphology and surface area does not influence subchondral bone density distribution in the dysfunctional sacroiliac joint

Amélie Poilliot (ajpoilliot@outlook.com)
University of Basel
Niels Hammer
Medical University of Graz
Mireille Toranelli
University of Basel
Max Hans-Peter Gay
University of Basel
Magdalena Müller-Gerbl
University of Basel

Research Article

Keywords: bone mineralisation, computed tomography, bone mineral density, Hounsfield units, osteoabsorptiometry, sacroiliac joint, sacroiliac joint dysfunction, sacroiliac morphology, subchondral bone plate

Posted Date: June 22nd, 2022

DOI: https://doi.org/10.21203/rs.3.rs-1760088/v1

Abstract

Background: The subchondral lamella of the sacroiliac joint (SIJ) auricular surface is morphologically inconsistent, varying inter-individually and side-dependently. These variations have been well documented, however, the morpho-mechanical relationship to sacroiliac joint dysfunction (SIJD) remains unstudied to date. Here, the bone mineralisation density of the iliac and sacral auricular surface subchondral endplate is compared between morphological subtypes, as well as in large and small surfaces, in a cohort comprising SIJD joints and controls.

Methods: Computed tomography (CT) datasets from 29 patients with bilateral or unilateral SIJD were subjected to CT osteoabsorptiometry. Sacral and iliac surface areas and posterior angles were calculated and surfaces were classified into small (<15 cm^3) and large (≥15 cm^3) joints and morphological types 1 (>160°), 2 (130-160°) and 3 (<130°), respectively. Mineralisation patterns were classified into four patterns, two marginal (M1 and M2) and two non-marginal (N1 and N2). Each sacral and iliac surface was subsequently classified into one of these mineralisation groups.

Results: The surface area of all joints in the cohort averaged 15.0±2.4 cm^2 (males 16.2±2.5 cm^2, females 13.7±1.6 cm^2). No age correlations with surface area were found nor differences in mean HU values when comparing sizes, sexes or morphology type when looking at painful joints (unilateral or bilateral) and contralateral non-painful joints. Comparisons of controls with the SIJD cohort revealed significant differences in female sacra (p=0.02) and small sacra (p=0.03). There was low conformity in marginal and non-marginal patterns, 26% for contralateral non-painful joints, and 46% conformity in painful joints. The majority of dysfunctional joints was of type 2 morphology (59%), equally distributed between small (49%) and large joints (51%). Larger joints had the highest frequency of painful joints (72%). Regarding the prominence of sub-patterns, M1C was more prominent in painful joints.

Conclusions: Load distribution related to difference in auricular surface morphology seems to have little impact on pain-related subchondral bone adaptation in cases of SIJD. Larger joints may be predisposed to the onset of pain due to the weakening of the extracapsular structures. Pain-affected joints reflect common conformity patterns of sacral apex mineralisation with corresponding superior corner iliac mineralisation.

Background

The morphology of the auricular surfaces of the sacroiliac (SIJ) has been studied in relation to the changes occurring in response to pelvic sexual dysmorphism [1–5] and the natural degeneration that the joint endures with time [2–8]. Some studies have looked into the influence of the morphological differences and the placement of the endplates in relation to the bony anatomy [6, 9, 10] to understand the role of the auricular endplate in joint mobility and bipedal force transmission. But, few studies have looked into whether the general shape and size of the SIJ auricular surface is associated with painful

conditions of the SIJ, such as sacroiliac joint dysfunction (SIJD), and what this might signify in relation to the detection and handling of the condition [5, 11–13].

The auricular surface (size and morphology) is variable, varying inter-individually, as well as side dependently even within the same person. Three dimensionally, the auricular surface is not flat but composed of ridges and grooves [14–16] allowing for the sacra and ilia to firmly interlock. Morphological studies have classified the shape of the surface based the measurement of the posterior angle [5, 8, 11, 17, 18] into three morphology types: type 1 (T1) has a wide posterior angle (> 160°), type 3 (T3) a narrow posterior angle (< 130°) and type 2 (T2) is in between (130–160°) [11, 19].

A previous paper [19] reports variation in size and shape of the auricular surface in a control cohort of SIJs and look into potential differences in subchondral bone (SCB) density. Results showed that size and morphology have little impact on the SCB density patterns, however, larger joints had higher mineralisation only seen on the iliac side [19]. Applying the same methods, this study aims to compare the mineralisation distribution between the three morphological types in a cohort of SIJ pain-affected joints. This will also be looked at when comparing joint size to see if that has an influence on mineralisation. The densitograms would allow visualising the mineralisation pattern across the surface which corresponds to the continuous loading conditions the joint endures. It will highlight the areas of high/low stress within the joint and thus provide information on the load dissipation within the painful state of the SIJ. It was hypothesised that joints with dysfunction will reflect pattern differences than non-dysfunctional joints in the superior and anterior parts of the surface

Materials And Methods

Specimens

Twenty-seven patient cases diagnosed with unilateral or bilateral SIJD (13 females; 14 males; range 26 to 79 years) were collected between 2009 and 2018 in the JCHO Sendai Hospital, Sendai, Japan. These patients have been used in previous studies [19, 20]. All patients identified the posterior superior iliac spine as the main pain area via a one-finger test [21] and following examination were considered to having SIJ pain. Definitive diagnosis of SIJD in these patients was confirmed by more than 70% pain relief after SIJ local anesthetic injections under fluoroscopic guidance [22]. Patients with a history of infection, tumors in the lumbopelvic area, recent lumbar spine and pelvic fractures, and seronegative spondylarthropathy were excluded. All included patients had a history of other injections including selective nerve root infiltration and/or lumbar disc nerve block that were negative.

In this study, the SIJD cohort was separated into the ‘painful’ joint cohort (all bilateral cases and the unilateral painful sides) and the painless joints (those with pain on the contralateral side) (Fig. 1). In addition, data corresponding to a group of control specimens (with no SIJ-related pain or pathology), used previously [23] were used for the final comparison of this study comparing the SIJD patients with the controls. This cohort was made up or body donors and patient CT scans (Fig. 1).

CT osteoabsorptiometry (CT-OAM)

Conventional clinical CT (SOMATOM as64 open, Siemens, Munich, Germany) data sets from patients were deployed as in previous studies [23, 24]. Slice thickness was 0.6 mm. Datasets were evaluated using an image analysis software (Analyze, v7.4, Biomedical Imaging Resource, Mayo Foundation, Rochester, NY, USA). Ilia and sacra were first manually segmented within the CT scans to reconstruct a three-dimensional lateral reconstruction of both bones before the subchondral endplate of both the sacrum and the ilium of each specimen was manually isolated. The maximum intensity projection revealed the Hounsfield Unit (HU) of each pixel of the endplate as a colormap [25] so that for every image point, each maximum density value of the underlying bone plate was projected onto the surface. Threshold values were ≤ 200 to ≥ 1200 HU chosen according to previous studies and displayed as colour-coded densitograms [26].

Classification into morphology types

Using ANALYZE, three-dimensional densitograms of the bones were oriented laterally to face the auricular surfaces. Inkscape v1.0.2-2 (The Inkscape Project, NY, USA; https://inkscape.org) was then used to calculate the alpha-angle for the classification of the surface into morphology T1, T2 and T3 based on the method developed by MK Jesse, C Kleck, A Williams, B Petersen, D Glueck, K Lind and V Patel [11]. The tree morphologies were as follows: T1 has a wide posterior angle (> 160°), T3 narrow posterior angle (< 130°) and T2 is in between (130–160°). The process involved making two lines through the centre of each limb and a third through the cross over point of the first two lines and the ‘centre’ of the angle at the posterior border [23]. The mean angle between the two limbs was then measured via the three points (Fig. 2).

Area classification

Classification of ‘large’ and ‘small’ joints was arbitrarily categorised based on the mean area of all the joints in the controls. ‘Small’ surfaces had an area lower than the mean area, ‘large’ joint surfaces had an area higher than the mean area.

Pattern classification methodology

As previously described in A Poilliot, N Hammer, M Toranelli, T Doyle, M Gay and M Müller-Gerbl [23], patterns were identified belonging to two main groups: the marginal (M) and non-marginal groups (N). This assessment was made based on a semi-quantitative analysis of the entire surface region colourmap of each joint surface. A pattern was marginal if 60–70% of the surface was less mineralised compared to the highly dense regions constituting the remaining 30–40%. The classification of the non-marginal patterns used the opposite criteria.

Statistical analysis

Prism (version 9.0.2, GraphPad, San Diego, CA, USA) was used for statistical analyses. Normal distribution of the data was determined using the Shapiro-Wilk test. Based on distribution, an ANOVA or a Kruskal-Wallis test was used to compare size differences and HU values between left and right sides as well as iliac and sacral sides between sexes. Age correlations were determined using a Pearson-r test. Dunn's post-hoc correction was not applied. *P* values of 0.05 or less were considered statistically significant. Values are given as mean values ± standard deviations with a 95% confidence intervals (CI). Correlation was defined as follows: strong ≥ 0.7, moderate 0.7 > r ≥ 0.5, weak 0.5 > r ≥ 0.1. For the semi-quantitative analyses, the patterns were classified into the four groups and percentages were formulated based on the amount in each category. Moreover, association between sub-patterns in each category was quantified using Cramér's Φ. Strong association Φ ≥ 0.5, moderate 0.5 > Φ ≥ 0.4, weak 0.4 > Φ ≥ 0.1 [27].

Intra- and inter-observer reliability for the pattern analysis was determined and assessed by two examiners (A.P. and M.P.). A.P repeated the classification four months after the first classification. Both judges were blinded to each other's' measurements. Using Cronsbach's α and a two-way, mixed intra-class correlation coefficient (ICC), a good result was set at ≥ 0.70, and ≥ 0.90 being excellent. A Cronbach's α intra-rater reliability result was 0.92, and an inter-rater reliability ICC result of 0.90 was found.

Results

Size does not correlate with age in painful joints, but there was a significance size difference between sexes

The surface area of the total SIJD cohort averaged 15.0 ± 2.4 cm^2 (95% CI: 14.5–15.7 cm^2); males 16.4 ± 2.3 cm^2 (95% CI: 15.6–17.21 cm^2), females 13.7 ± 1.6 cm^2 (95% CI: 13.1–14.2 cm^2). In all painful joints (unilateral and bilateral cases combined), a significant size difference was observed between sexes ($p <$ 0.01 sacra and ilia) (Fig. 3A). Furthermore, no significant differences were found in mean sacrum and ilium mineralisation density when comparing sizes (ilia, small 721 ± 155 HU (95% CI:), large 757 ± 114 HU (95% CI:); sacra, small 579 ± 109 HU (95% CI:), large 601 ± 131HU (95% CI:)), sexes (ilia, males 714 ± 121 HU (95% CI:), females 768 ± 144 HU (95% CI:); sacra, males 579 ± 139 HU (95% CI:), females 600 ± 96 HU (95% CI:)), or morphology T1 and T2 (ilia T1, 736 ± 149 HU (95% CI:), T2, 747 ± 127 HU (95% CI:); sacra: T1, 609 ± 136 HU (95% CI:), T2, 579 ± 113 HU (95% CI:)). No age correlations with joint surface area were found in painful joints (p = 0.2, sacra; p = 0.7, ilia).

Bilaterally and unilaterally painful joints show no differences in size nor morphology-related mineralisation density

As a consequence of the low onset of joint morphology T3, only comparisons between T1 and T2 were made. In the bilaterally painful joints, no significant size difference was present between sexes (p = 0.08 sacra; p = 0.3 ilia) (Fig. 3B). Furthermore, no significant differences were found in mean sacrum and ilium mineralisation density when comparing sizes (ilia, small 682 ± 130 HU (95% CI:), large 768 ± 84 HU (95% CI:); sacra, small 575 ± 84 HU (95% CI:), large 648 ± 163 HU (95% CI:)), sexes (ilia, males 682 ± 130 HU

(95% CI:), females 768 ± 84 HU (95% CI:); sacra, males 575 ± 84 HU (95% CI:), females 648 ± 163 HU (95% CI:)), or morphology T1 and T2 (ilia, T1 748 ± 103 HU (95% CI:), T2 727 ± 125 HU (95% CI:); sacra: T1 688 ± 137 HU (95% CI:), T2 555 ± 100 HU (95% CI:)).

In unilaterally painful joints, a significant size difference was observed between sexes ($p < 0.03$ sacra and ilia) (Fig. 3C). No significant difference was found in mean sacrum and ilium mineralisation density when comparing sizes (ilia, small 751 ± 173 HU (95% CI:), large 747 ± 140 HU (95% CI:); sacra, small 583 ± 134 HU (95% CI:), large 568 ± 98 HU (95% CI:)), sexes (ilia, males 722 ± 128 HU (95% CI:), females 779 ± 178 HU (95% CI:); sacra, males 554 ± 105 HU (95% CI:), females 598 ± 124 HU (95% CI:)), or morphology T1 and T2 (ilia, T1 730 ± 173 HU (95% CI:), T2 770 ± 133 HU (95% CI:); sacra: T1 531 ± 85 HU (95% CI:), T2 595 ± 122 HU (95% CI:)).

Unilateral SIJD yielded no size, sex nor morphology-related mineralisation difference to non-painful joints nor bilateral SIJD

Comparison of cases with unilateral pain with their contralateral non-painful side yielded no significant size differences (Fig. 4A,B,C). Mineralisation was indifferent when comparing sexes, sizes and morphology T1 and T2. No significant difference was found between bilateral and unilateral painful joints when comparing mean HU mineralisation between sex, size and morphology T1 and T2 (Fig. 4A,B,C).

Sacrum mineralization in females with SIJD pain is different when compared to the SIJ of healthy controls

Significant differences in mineralization was found between healthy controls and the painful joints from the SIJD cohort. These were found only in females, small joints and T2 joints only on the sacral side (Fig. 5). Furthermore, correlations between mean surface mineralisation and surface area reveal weak positive correlations on the iliac side in both males and females in the control cohort (Fig. 6A) and bilaterally painful joints (Fig. 6B).

Semi-quantitative assessment of all sacroiliac joint surfaces revealed four main patterns for the purpose of classification

Two of these were marginal patterns: M1 had mineralisation located around the anterior border which could include the superior corner and/or apex and pattern M2 had mineralisation scattered around the borders with no specific maxima, the centre region demineralised. The other two were non-marginal patterns: pattern N1 had mineralisation spread over the whole superior region, pattern N2 had mineralisation spread over the superior and anterior regions (Fig. 7).

Pattern M1 was subdivided into four sub-patterns (Fig. 8) based on the visual assessment of the highest mineralisation point (maxima) at the anterior border. Pattern A had mineralisation across the anterior border. Pattern B had a maximum located in the superior corner only. Pattern C had maxima in the superior corner and apex. Pattern D had a maximum at the apex.

Painful joints exhibit higher pattern conformity in corresponding sacra and ilia than those without pain

A joint is 'conforming' when the sacral and iliac articulating surfaces reflect the same pattern. For the painful joints, there was 46% conformity between patterns M1 to N2, and 6% with the M1 sub-patterns. Conformity was higher than compared to the controls (M1 to N2: 26%; M1 sub-pattern added: 5%). The majority of dysfunctional joints was of T2 morphology (59%), and was equally distributed between small (49%) and large joints (51%). The majority of non-painful joints was also of T2 morphology (53%) and had smaller surface areas (63%) (Table 1). From a different perspective, within each morphology type, T1 and T2 had a majority of painful joints (both > 60%), with T3 having close to equal painful and non-painful joints. Larger joints had the highest frequency of painful joints (72%).

Table 1

Distribution of painful and non-painful joints by morphology type and auricular surface size. Type 1 morphology: posterior angle (> 160°), type 2 morphology: posterior angle (130–160°), type 3 morphology: posterior angle (< 130°).

	Morphology			**Small joints**		**Large joints**	
				n = 58		**n = 50**	
	Type 1	**Type 2**	**Type 3**	**Females**	**Males**	**Females**	**Males**
	n = 43	**n = 61**	**n = 4**				
Painful joints n = 70	27 (38%)	41 (59%)	2 (3%)	27 (39%)	7 (10%)	7 (10%)	29 (41%)
Non-painful joints n = 38	16 (42%)	20 (53%)	2 (5%)	15 (39%)	9 (24%)	3 (8%)	11 (29%)

Regarding the prominence of sub-patterns, M1C was more prominent in painful joints (39%), whilst pattern M1A was more frequent in the controls (31%) (Table 2). When comparing ilia and sacra in painful joints, M1B sub-pattern was more common in the ilia (> 55%) whilst M1C was most common in the sacra (> 60%). Cramér's Φ revealed strong associations between patterns M1A and M1C in all painful joints and associated sub cohorts as well as in the controls (Table 2). Unilaterally and bilaterally painful joints were similarly associated with all three sub- patterns (Table 2).

Table 2

Results of Cramér's Φ association between sub-patterns, M1A, M1B and M1C in each category. Strong association Φ ≥ 0.5, moderate 0.5 > Φ ≥ 0.4, weak 0.4 > Φ ≥ 0.1.

Cohort	n	Sub-pattern distribution			Cramér's Φ		
		M1A	M1B	M1C			
All painful joints	44	34%	27%	39%	Φ = 0.73		
Controls	171	31%	14%	25%	$p <$ 0.01	Φ = 0.71	
Non-painful joints (but painful contralateral side)	22	59%	9%	32%		$p <$ 0.01	Φ = 0.73
Unilaterally dysfunctional joints	27	37%	22%	41%	Φ = 0.71		$p <$ 0.01
Bilaterally dysfunctional joints	17	30%	35%	35%	$p <$ 0.01		

Discussion

This study semi-quantitatively analysed the mineralisation patterns of the sacral and iliac auricular surfaces of the SIJ in SIJD-affected patients. It provides insights into the influence of surface size and shape in morpho-mechanical differences between individuals. The results presented here are likely representative of the long-term loading conditions of the which demonstrate the biomechanical stresses applied to the SIJ when subjected to dysfunction.

Dysfunctional joints have more commonly larger SIJ surface areas

Joint pain was previously associated more with T3 (acute angle) morphology where authors hypothesised that a relative decrease in surface area available for dissipation was present in T3, compared to the more obtuse T1 and T2 (more surface for force dissipation) [11]. Therefore, pain could be caused by increased force transmission to the ligaments and periarticular structures. T1 is more ovoid and might allow more transmission over the surface preventing excess forces from reaching the ligamentous structures so causing less pain [11]. Our study here however, does not produce conclusive results for painful joints with T3 morphology as there were too few to reliably assess the mineralisation pattern. When looking at the patterns corresponding to painful joints in the SIJD cohort, the majority of large surfaces were painful. These findings suggest that larger joints are predisposed to develop pain, which may be due to the dysfunction of extracapsular joint structures which take active part in pelvic load distribution (i.e.: ligaments, cartilage, fat etc.) [28]. As there is more surface to dissipate loads in 'large joints' this would require less dissipation via extracapsular structures which may result in a certain

weakness of these compared to those in ‘smaller’ joints. This may be why larger joints are predisposed to pain. In addition, larger bones and joints often belong to patients with greater height and males which may then result in an increase of stresses to be dissipated within the SIJ with motion [5, 11].

In addition, comparisons between the controls and the SIJD cohort revealed significant differences in total surface mineralisation density in smaller joints and in females only on the sacral side. This may be caused by the sexual dimorphism seen where females retain more mobility in their joints for childbearing and it was also shown that females had in consequence, smaller joints for that purpose [23, 29]. Previous studies have demonstrated the potential for the sacrum to become more stressed in dysfunctional cases [19].

Conformity may be an indicator of painful sacroiliac joints

When comparing the conformity of patterns in corresponding surfaces, this reflected higher conformity in painful joints than in the pain-free state. This was expected, as a previous study has shown that the inferior region of the SIJ shows similar mineralisation density in the painful state [19]. Semi-quantitative pattern analysis has shown that mineralisation distribution of patterns in corresponding sacral and iliac surfaces is more likely to be similar in painful than in non-painful joints. Regarding pattern distribution in painful joints, there was a trend towards higher mineralisation in the apex (pattern M1C), whilst the controls have more commonly maximum mineralisation in the anterior region (pattern M1A). Regarding extent of the conformity to a sub-pattern level, the study revealed that in the joints

showing an M1 conformity, there was a trend towards a specific pattern-combination: apex mineralisation on the sacrum (M1C) with corresponding superior corner mineralisation on the ilium (M1B). This may show, to some extent, the chronic adaptation of the joint to pain where the sacral surface shows a similar mineralisation distribution to the iliac surface as showed previously [19]. Non-conformity may be due to structural properties and the dampening of surrounding supportive tissues. If this tissue cannot perform correctly, there is a direct transference of forces which leads to conformity. So, conformity could be a sign of stabilisation tissue weakness, which could be an underlying reason for pain.

Painful joints reflect variable mineralisation patterns compared to controls

Previous results show that morphology likely does not affect mineralisation patterns at the SIJ in the ‘healthy’ state, however, size may be a factor. In fact, it was shown that larger joints reflected higher mineralisation patterns than smaller joints only on the iliac side. It was hypothesised that this may be due to cartilage thinning on the iliac side which may account for a mineralisation ‘compensation mechanism’ for the loss of chondral tissue [23]. In this study, it was found that mean mineralisation in the painful joint cohort was higher in females/ small joints on the sacral side when compared to the controls. As female joints tend to be smaller than male joints, they require more dampening of forces are therefore more prone to higher densities across the surface. Furthermore, mean mineralisation positive correlations with

size were revealed in the controls and bilaterally painful joints on the iliac side in both males and females and a negative correlation on the sacral side in females in the painful joint cohort, specifically in unilaterally painful joints. These results reflect previous results where larger joints reflect higher mineralisation patterns than smaller joints only on the iliac side, as do bilaterally painful joints which may reflect the similar walking mechanisms in the pain less state as the bilaterally painful state.

In the control cohort, when assessing the mineralisation maxima zone differences using the sub-patterns, all sub-groups (albeit T3 sacra) showed M1A (anterior surface) sub-pattern majority. This suggests that mineralisation maxima zones are not affected by size, shape, sex nor bone. However, when assessing the SIJD joints both painful and non-painful sides, a variability in patterns was observed compared to the control cohort. The SIJD cohort revealed that morphology did not seem to affect the patterns as all sacra had a majority of pattern M1C and the ilia M1B in the painful joints. Respectively the painful and non-painful state did not play a role. However, size may have had an effect with larger joints having a majority of anterior border mineralisation (M1A) and smaller joints having a majority of apex mineralisation (M1C). This again may reflect the need for larger joints to compensate for the extracapsular structures and show a broader subchondral mineralisation across the surface than ‘smaller’ joints. Non-painful joints had variable patterns from the control cohort but these were similar to those found in the painful state. In fact, Cramér’s Φ revealed significant associations between surface sub-patterns and a particular cohort where M1A and M1C were the most frequent sub-patterns in the painful joints, controls and non-painful SIJD joints. Bilaterally and unilaterally painful joints revealed close to equal frequencies of all three sub patterns. This suggests that sub-patterns are likely not indicative of the pain status of the joint nor type of dysfunction (unilateral/bilateral pain). Therefore, our hypothesis stating that joints with dysfunction would reflect pattern differences than those of the control group can only be partly accepted. This similarity with the painful state suggests that the SCB mineralisation evolves in a similar way on both sides independent of pain, suggesting that pain is not directly related to bone mineralisation density.

Regarding the limitations of the study, the manual calculation of the posterior angle was performed by only one investigator. T3 morphology had too few values to reliably compare with the other two morphologies so was often excluded from comparisons. Anatomical variants were not accounted for and may have had some influence on joint area [30]. The study does not account for population difference and potential variables between the two cohorts compared: controls and SIJD patients.

Conclusions

Load distribution related to auricular surface morphological differences seems to have little impact on pain-related SCB adaptation in cases of sacroiliac joint dysfunction. Larger joints may be predisposed to develop pain due to the weakening of the extracapsular structures directly related to the surface size. Painful joints reflect common conformity patterns of sacral apex mineralisation with corresponding superior corner iliac mineralisation which could be a sign of structural weakening within the joint.

Declarations

Ethics approval and consent to participate

The Institute Review Board of JCHO Sendai Hospital, Sendai, Miyagi, Japan (no. 2019-1) approved the present study. Institutional approval was acquired for the use of patient datasets used in research studies for diagnostic and therapeutic purposes. Approval was granted on the grounds of existing datasets. Informed oral consent was obtained from all participants of this study. All methods were carried out in accordance with relevant guidelines and regulations. All the data were analyzed anonymously.

Consent for publication

Not applicable

Availability of data and materials

All data generated or analysed during this study are included in this published article and its supplementary information files.

Competing interests

The authors declare that they have no competing interests.

Funding

The author(s) received no specific funding for this work.

Author contributions

A.P. wrote the first draft of the manuscript, created the figures and collected and analysed the data. A.P. and M.M. both worked on conceptualising and formulating the methodology. M.T. provided technical support for the analysis of some patients. M.G., N.H. and M.M. reviewed the manuscript

Acknowledgements

We acknowledge support from the Dr Daisuke Kurosawa of JCHO Sendai Hospital, Sendai, Japan for providing the authors with the specimens with SIJ dysfunction and Professor Terence Doyle from the University of Otago, New Zealand for the control patient scans. The authors would like to thank and acknowledge the patients who contributed to this research project and extend their gratitude to the body donors for their contribution to this project.

References

1. Bonczarowska JH, Bonicelli A, Papadomanolakis A, Kranioti EF: **The posterior portion of the ilium as a sex indicator: A validation study**. Forensic Science International 2019, **294**.

2. Valojerdy MR, Hogg DA: **Sex differences in the morphology of the auricular surfaces of the human sacroiliac joint**. Clin Anat 1989, **2**(2):63–67.
3. Anastasiou E, Chamberlain AT: **The sexual dimorphism of the sacro-iliac joint: an investigation using geometric morphometric techniques**. J Forensic Sci 2013, **58 Suppl 1**:S126-134.
4. Rmoutilova R, Dupej J, Veleminska J, Bruzek J: **Geometric morphometric and traditional methods for sex assessment using the posterior ilium**. Leg Med (Tokyo) 2017, **26**:52–61.
5. Nishi K, Saiki K, Oyamada J, Okamoto K, Ogami-Takamura K, Hasegawa T, Moriuchi T, Sakamoto J, Higashi T, Tsurumoto T *et al*: **Sex-based differences in human sacroiliac joint shape: a three-dimensional morphological analysis of the iliac auricular surface of modern Japanese macerated bones**. Anat Sci Int 2019.
6. Brunner C, Kissling R, Jacob H: **The effects of morphology and histopathology findings on the mobility of the sacroiliac joint**. Spine (Phila Pa 1976) 1991, **16**(9):1111–1117.
7. Nishi K, Saiki K, Imamura T, Okamoto K, Wakebe T, Ogami K, Hasegawa T, Moriuchi T, Sakamoto J, Manabe Y *et al*: **Degenerative changes of the sacroiliac auricular joint surface-validation of influential factors**. Anat Sci Int 2017, **92**(4):530–538.
8. Nishi K, Tsurumoto T, Okamoto K, Ogami-Takamura K, Hasegawa T, Moriuchi T, Sakamoto J, Oyamada J, Higashi T, Manabe Y *et al*: **Three-dimensional morphological analysis of the human sacroiliac joint: influences on the degenerative changes of the auricular surfaces**. J Anat 2018, **232**(2):238–249.
9. Waldrop JT, Ebraheim NA, Yeasting RA, Jackson WT: **The location of the sacroiliac joint on the outer table of the posterior ilium**. J Orthop Trauma 1993, **7**(6):510–513.
10. Rana SH, Farjoodi P, Haloman S, Dutton P, Hariri A, Ward SR, Garfin SR, Chang DG: **Anatomic evaluation of the sacroiliac joint: A radiographic study with implications for procedures**. Pain Physician 2015, **18**(6):583–592.
11. Jesse MK, Kleck C, Williams A, Petersen B, Glueck D, Lind K, Patel V: **3D Morphometric Analysis of Normal Sacroiliac Joints: A New Classification of Surface Shape Variation and the Potential Implications in Pain Syndromes**. Pain Physician 2017, **20**(5):E701-E709.
12. Ou-Yang DC, York PJ, Kleck CJ, Patel VV: **Diagnosis and management of sacroiliac joint dysfunction**. J Bone Joint Surg Am 2017, **99**(23):2027–2036.
13. Beal MC: **The sacroiliac problem: Review of anatomy, mechanics, and diagnosis**. J Am Osteopath Assoc 1982, **81**(10):667–679.
14. Snijders CJ, Vleeming A, Stoeckart R: **Transfer of Lumbosacral Load to Iliac Bones and Legs.1. Biomechanics of Self-Bracing of the Sacroiliac Joints and Its Significance for Treatment and Exercise**. Clin Biomech (Bristol, Avon) 1993, **8**(6):285–294.
15. Forst SL, Wheeler MT, Fortin JD, Vilensky JA: **The sacroiliac joint: Anatomy, physiology and clinical significance**. Pain Physician 2006, **9**(1):61–68.
16. Puhakka KB, Melsen F, Jurik AG, Boel LW, Vesterby A, Egund N: **MR imaging of the normal sacroiliac joint with correlation to histology**. Skeletal Radiol 2004, **33**(1):15–28.

17. Schunke B, Bernard G: **The anatomy and development of the sacro-iliac joint in man**. Anat Rec 1938, **72**(3):313–331.
18. Weisl H: **The articular surfaces of the sacro-iliac joint and their relation to the movements of the sacrum**. Acta Anat (Basel) 1954, **22**(1):1–14.
19. Poilliot A, Doyle T, Kurosawa D, Toranelli M, Zhang M, Zwirner J, Müller-Gerbl M, Hammer N: **Computed tomography osteoabsorptiometry-based investigation on subchondral bone plate alterations in sacroiliac joint dysfunction**. Sci Rep 2021, **11**:8652.
20. Poilliot A, Kurosawa D, Toranelli M, Zhang M, Zwirner J, Müller-Gerbl M, Hammer N: **Subchondral bone changes following sacroiliac joint arthrodesis – a morpho-mechanical assessment of surgical treatment of the painful joint**. Pain Physician 2021, **24**(3):E317-E326.
21. Murakami E, Aizawa T, Noguchi K, Kanno H, Okuno H, Uozumi H: **Diagram specific to sacroiliac joint pain site indicated by one-finger test**. J Orthop Sci 2008, **13**(6):492–497.
22. Murakami E, Kurosawa D, Aizawa T: **Treatment strategy for sacroiliac joint-related pain at or around the posterior superior iliac spine**. Clin Neurol Neurosurg 2018, **165**:43–46.
23. Poilliot A, Hammer N, Toranelli M, Doyle T, Gay M, Müller-Gerbl M: **Influence of size and shape of the auricular surfaces on subchondral bone density distribution in the sacroiliac joint** *Submitted* 2022.
24. Poilliot A, Tannock M, Zhang M, Zwirner J, Hammer N: **Quantification of fat in the posterior sacroiliac joint region applying a semi-automated segmentation method**. Comput Meth Prog Bio 2020, **191**:105386.
25. Johnston JD, Kontulainen SA, Masri BA, Wilson DR: **A comparison of conventional maximum intensity projection with a new depth-specific topographic mapping technique in the ct analysis of proximal tibial subchondral bone density**. Skeletal Radiol 2010, **39**(9):867–876.
26. Leumann A, Valderrabano V, Hoechel S, Gopfert B, Müller-Gerbl M: **Mineral density and penetration strength of the subchondral bone plate of the talar dome: high correlation and specific distribution patterns**. J Foot Ankle Surg 2015, **54**(1):17–22.
27. Cohen J: **Statistical Power Analysis for the Behavioral Sciences**, 2nd Edition edn. New York: Routledge; 1988.
28. Hammer N, Steinke H, Lingslebe U, Bechmann I, Josten C, Slowik V, Böhme J: **Ligamentous influence in pelvic load distribution**. Spine J 2013, **13**(10):1321–1330.
29. Derry DE: **The Influence of Sex on the Position and Composition of the Human Sacrum**. J Anat Physiol 1912, **46**(2):184–192.
30. Ziegeler K, Kreutzinger V, Diekhoff T, Roehle R, Poddubnyy D, Pumberger M, Hamm B, Hermann KGA: **Impact of age, sex, and joint form on degenerative lesions of the sacroiliac joints on CT in the normal population**. Sci Rep 2021, **11**(1):5903.

Figures

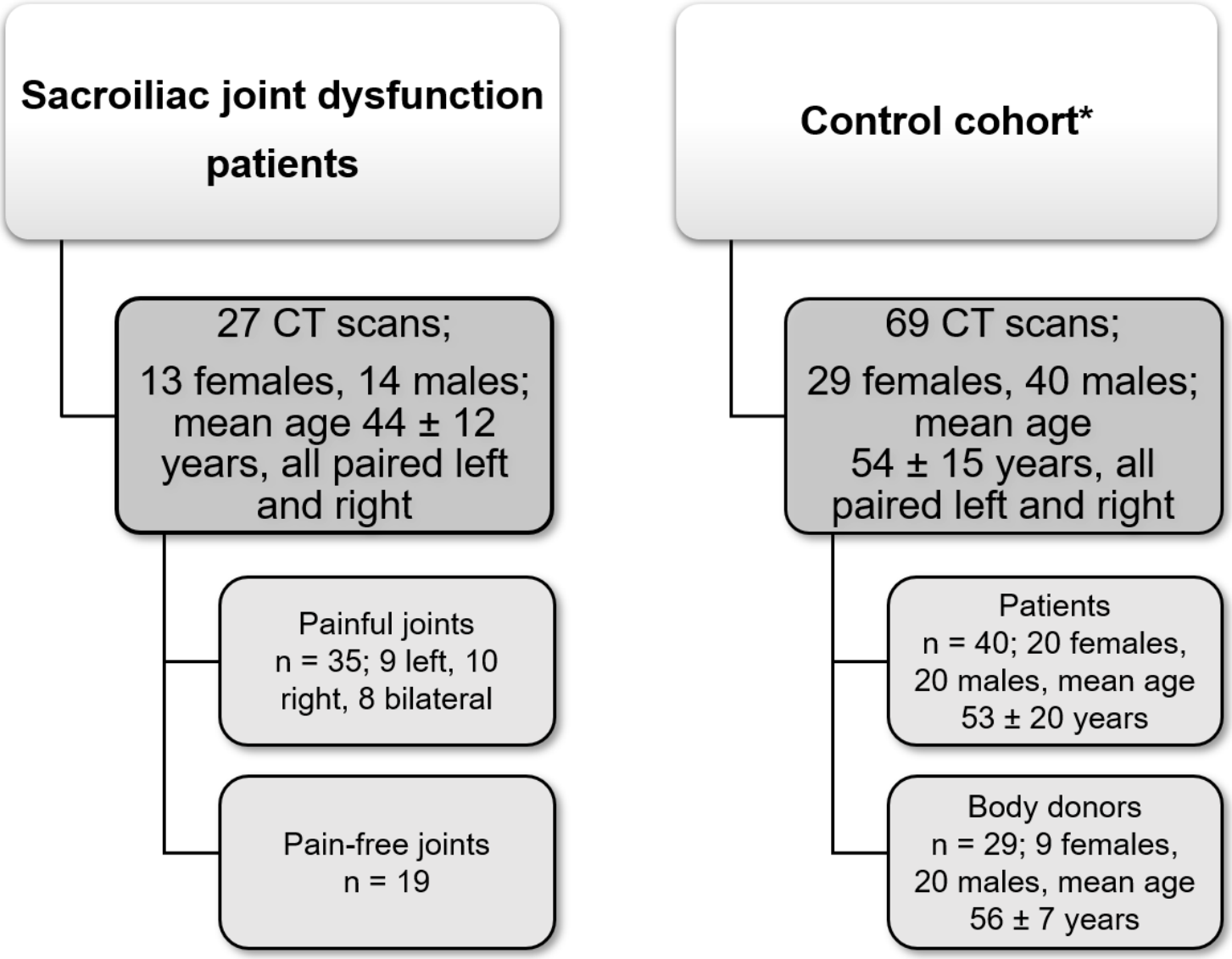

Figure 1

*Schematic representation of the materials used for the study. *None of these cases had a current or past history of low back pain, sacroiliac joint-related pathology or abnormalities on previous medical records and visible sacroiliac joint conditions visible on the CT (computed tomography) scans. This cohort was previously used in A Poilliot, N Hammer, M Toranelli, T Doyle, M Gay and M Müller-Gerbl [23].*

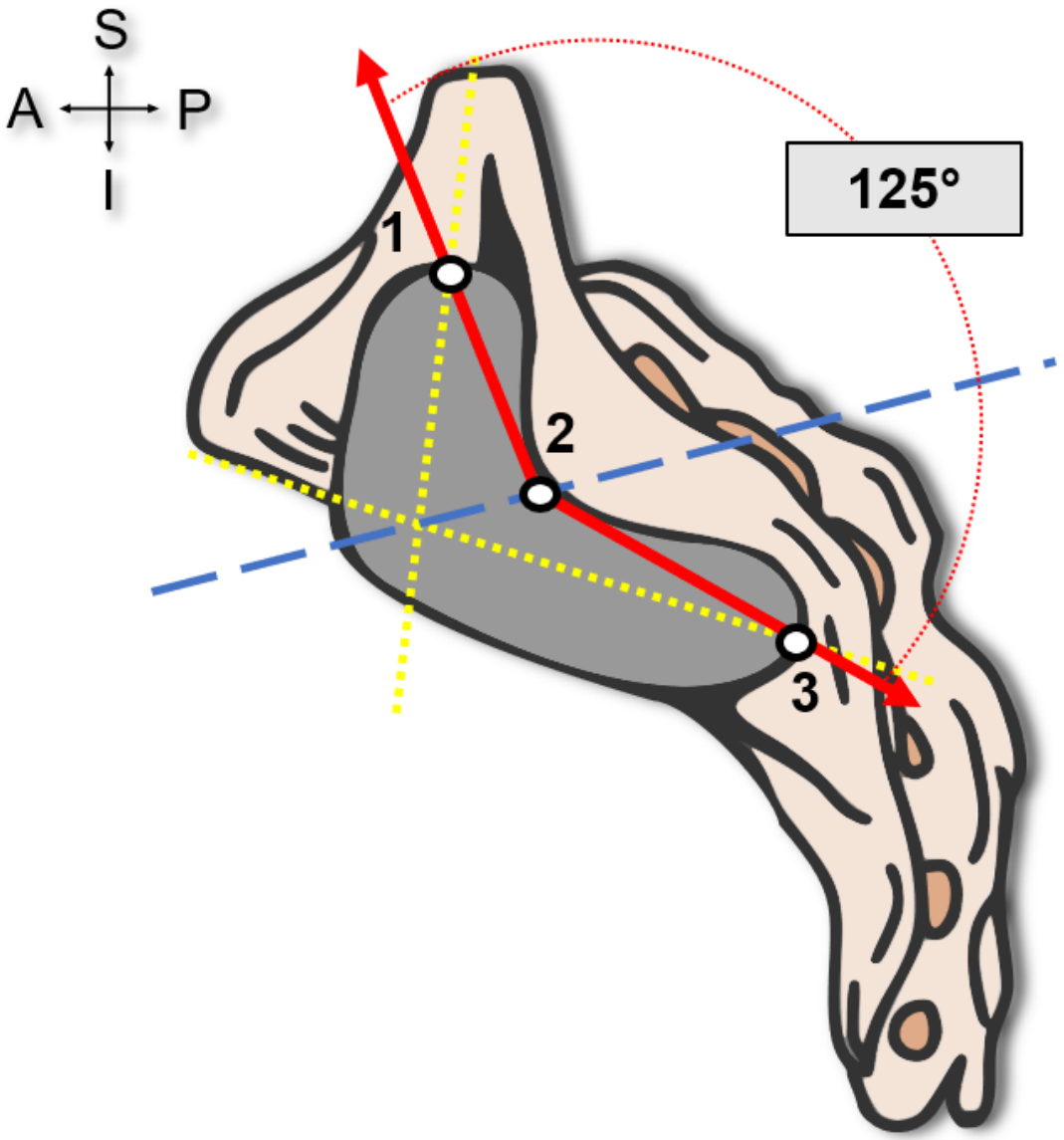

Figure 2

Schematic representation of the method for the posterior angle calculation using Inkscape. Yellow dotted lines: perpendicular through the centre of both limbs (points 1 and 3), blue dashed line: through the crossover point of the yellow lines and centre of the posterior angle (point 2). The posterior angle is measured between points 1, 2 and 3. A: anterior, I: inferior, P: posterior, S: superior.

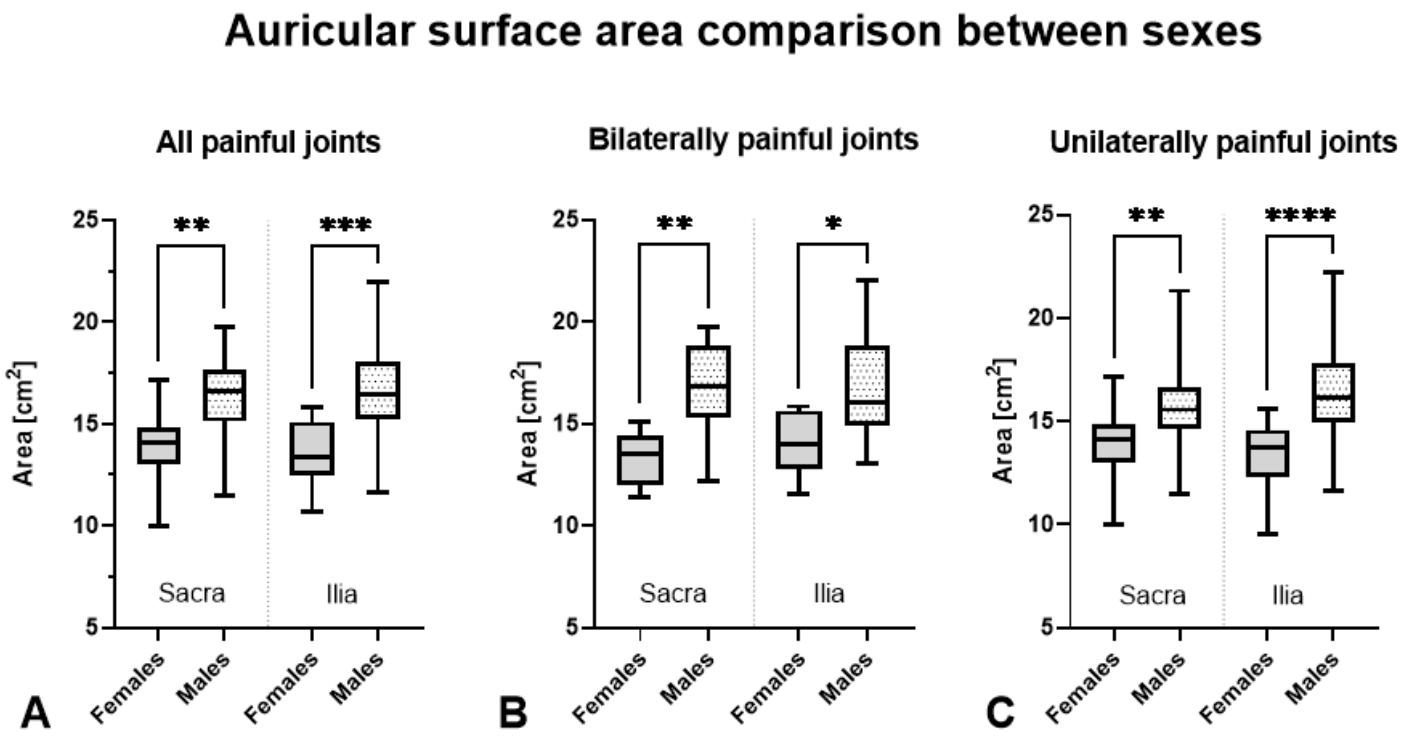

Figure 3

Auricular surface area comparisons between sexes in (A) all painful joints, (B) bilaterally painful joints and (C) unilaterally painful joints. The outlines of the boxes indicate the 25- and 75-percentile, the solid black horizontal line, the median. Whiskers indicate the minima and maxima. The dotted lines separate the sacra from the ilia in the table

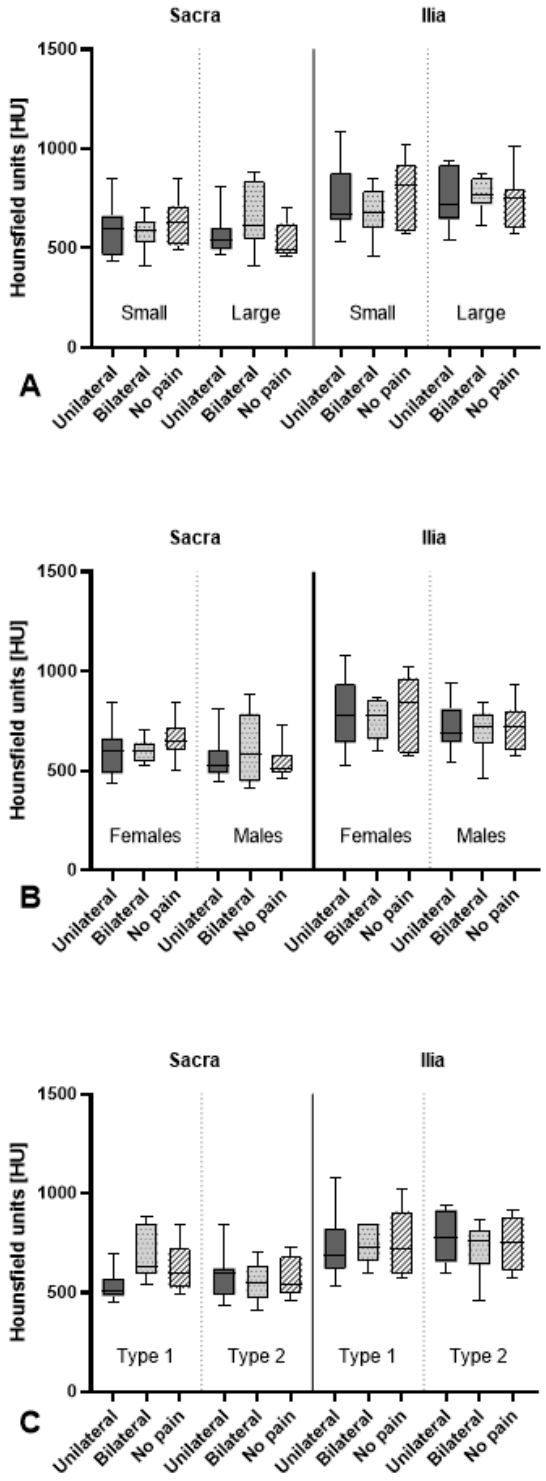

Figure 4

Box plot comparison between the unilaterally painful joints, bilaterally painful joints and the contralateral non-painful side (no pain) from the SIJD cohort. (A) Size comparison, (B) sex comparison, (C) morphology comparison between types 1 and 2 (too few values were available for an accurate type 3 comparison. The outlines of the boxes indicate the 25- and 75-percentile, the solid black horizontal line, the median. Whiskers indicate the minima and maxima. The dotted lines separate the sacra from the ilia

in the table. The thicker black line separates the sacra from the ilia values. Significance is considered as p < 0.05, with brackets illustrating this.

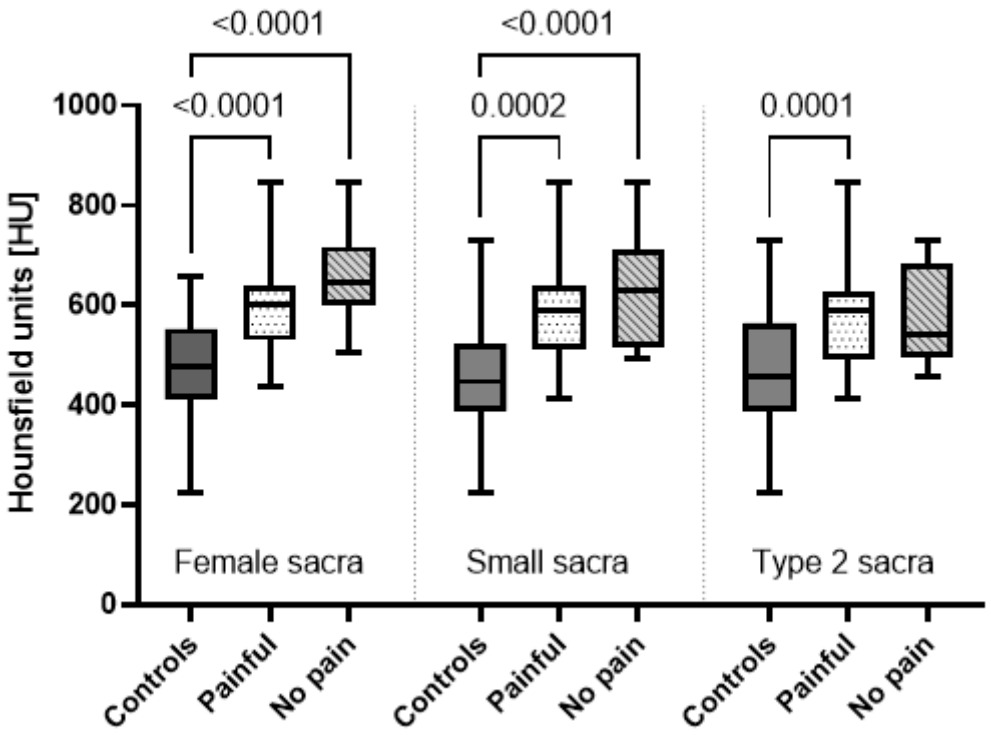

Figure 5

Box plot comparison between the control cohort, painful joints from SIJD cohort and contralateral non-painful side (no pain) also from the SIJD cohort. The outlines of the boxes indicate the 25- and 75-percentile, the solid black horizontal line, the median. Whiskers indicate the minima and maxima. The dotted lines separate the sacra from the ilia in the table. Significance is considered as p < 0.05, with brackets illustrating this.

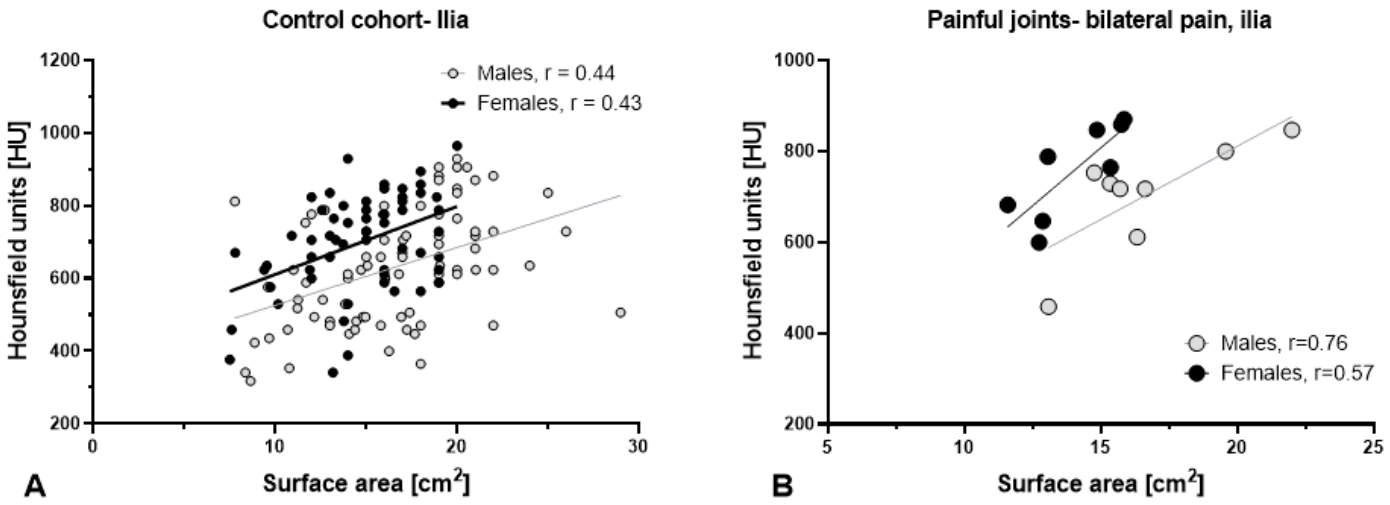

Figure 6

Significant correlations between auricular surface area and mean mineralisation in male and female ilia and sacra in both (A) the control, (B) joints with bilateral pain

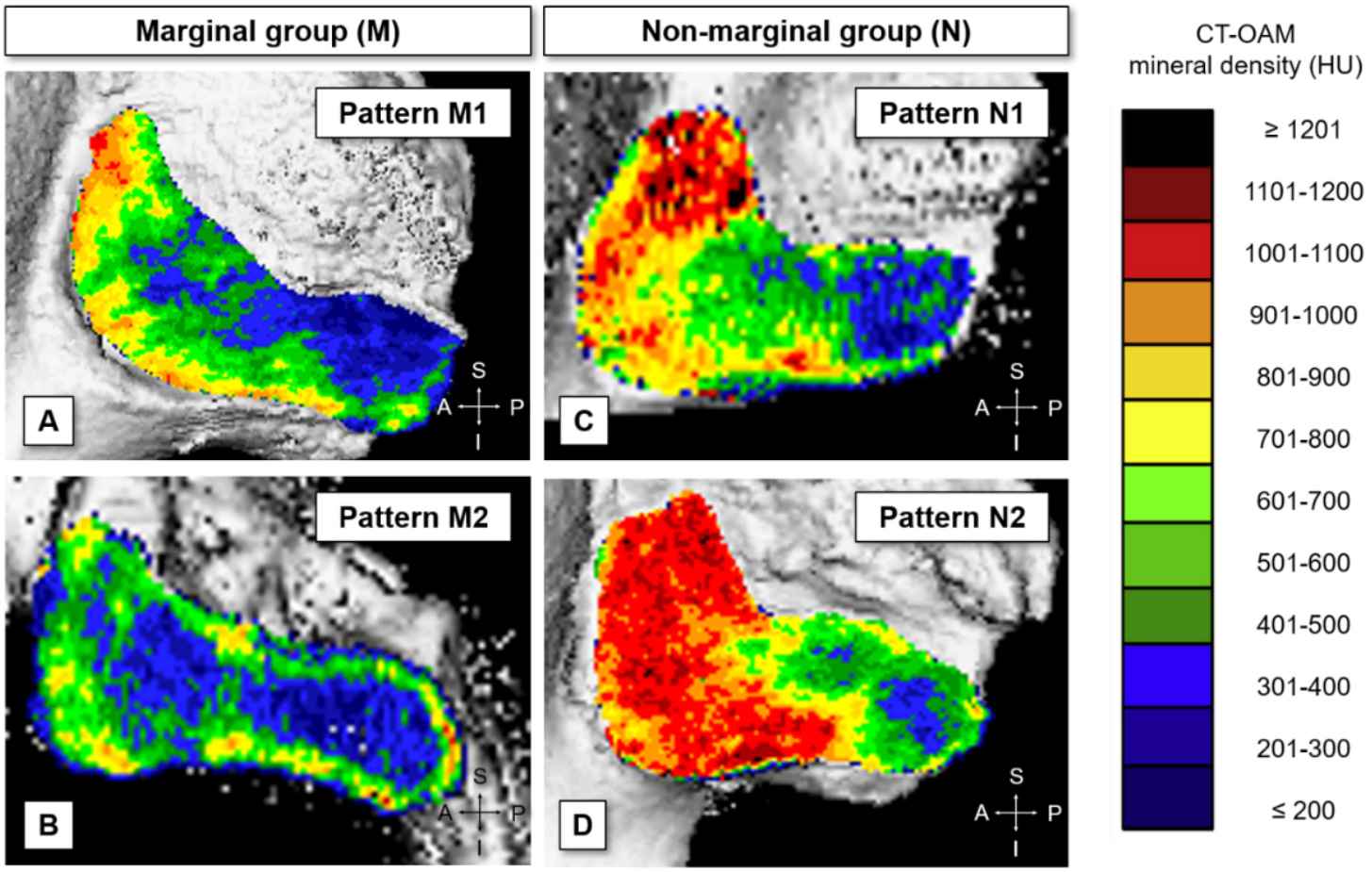

Figure 7

Pattern classification into the marginal and non-marginal groups (A) Pattern M1 (low mineralisation in >60% of the surface) with anterior border mineralisation. (B) pattern M2 with mineralisation around the borders. (C) Pattern N1 (high mineralisation in >60% of the surface) with mineralisation located in the superior corner. (D) Pattern N2 with mineralisation located in the superior corner and apex. On the right is the colourmap scale based on the Hounsfield Units (HU). A: anterior, I: inferior, M: marginal, N: non-marginal, P: posterior, S: superior.

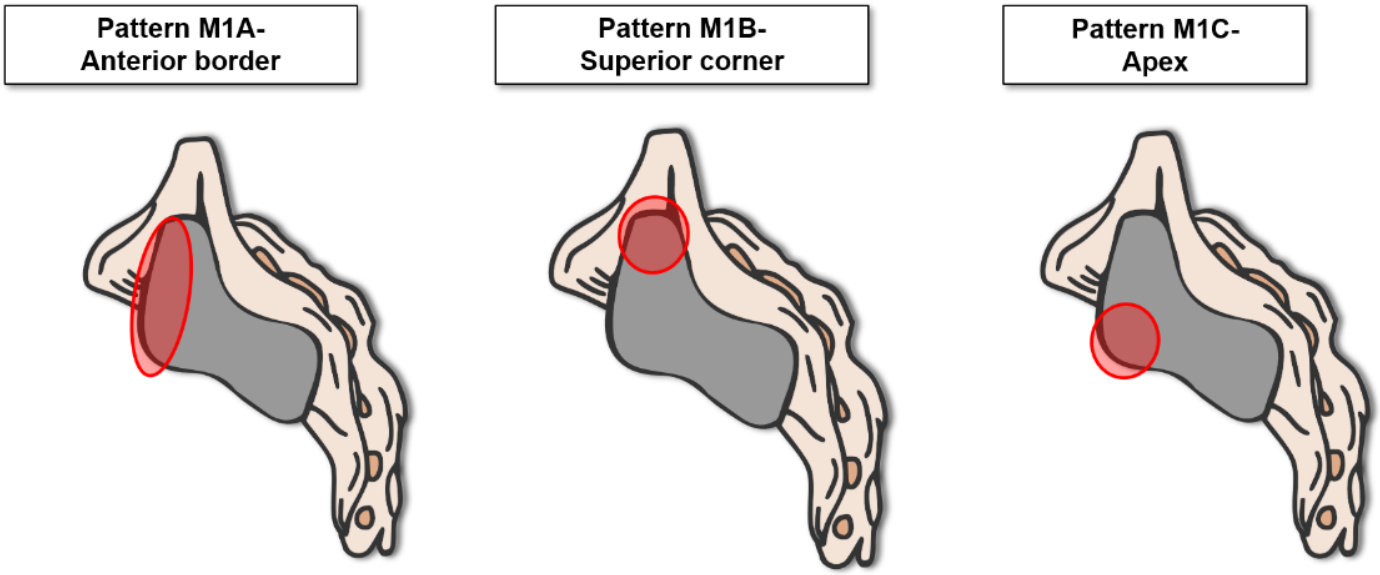

Figure 8

Classification of the morphology types of the auricular surface subchondral bone plate into the three sub-group patterns. Red circles represent the highly mineralised region. M1: marginal pattern 1

Supplementary Files

This is a list of supplementary files associated with this preprint. Click to download.

- SupportinginformationNEW.docx